Food Chemistry: X 24 (2024) 101919

Contents lists available at ScienceDirect

Food Chemistry: X

journal homepage: www.sciencedirect.com/journal/food-chemistry-x

Investigation of physicochemical properties and structure of ball milling pretreated modified starch-ferulic acid complexes

Zongwei Hao [a], Shengjun Han [a], Zhongyun Zhao [a], Zongjun Wu [a], Hui Xu [a], Chao Li [a], Mingming Zheng [a,b], Yibin Zhou [a], Yiqun Du [a,*], Zhenyu Yu [a,*]

[a] Key Laboratory of Jianghuai Agricultural Product Fine Processing and Resource Utilization, Ministry of Agriculture and Rural Affairs, Anhui Engineering Research Center for High Value Utilization of Characteristic Agricultural Products, State Key Laboratory of Tea Plant Biology and Utilization, College of Food and Nutrition, Anhui Agricultural University, Hefei 230036, China

[b] Key Laboratory of Oilseeds Processing, Ministry of Agriculture and Rural Affairs, Wuhan 430062, China

ARTICLE INFO

Keywords:
Ferulic acid
Starch
Multi-scale structure
Lower digestion efficiency
Density functional theory calculations

ABSTRACT

In this study, the formation mechanism, physicochemical properties, and intermolecular interactions of ball milling pretreated high amylose corn starch (HACS)-ferulic acid (FA) complexes were elucidated by density functional theory (DFT) calculations, and examined their structural and digestive properties. The results showed that the average molecular weight decreased to 92.155 kDa during ball milling pretreatment. The complexation degree of the ball milling pretreated HACS-FA complexes was increased, the relative crystallinity was increased by 11.74 %, and the short-range ordering was significantly improved. Notably, the content of single helix and double helix showed an increasing trend, indicating that HACS-FA complexes had a more compact V-type structure, which corresponded to a 22.39 % increase in resistant starch. DFT calculations further showed that the intermolecular interactions between HACS and FA were mainly hydrophobic, hydrogen bonding, and van der Waals forces. This study is expected to provide a new method for the efficient preparation of HACS-FA complexes.

1. Introduction

Starch is a plant polysaccharide found widely in cereal grains, corn, wheat, and other plants, which is the main source of daily carbohydrate intake for humans (Li et al., 2018; Liu et al., 2021). It consists mainly of amylose of a linear polymer (linked by α-1,4 glycosidic bonds) and amylopectin of a branched polymer (linked by α-1,4 and α-1,6 glycosidic bonds) (Zhang et al., 2021). In addition, different starch sources, amylose/amylopectin ratio, and structure all have a great effect on their digestibility (Li, 2023). Based on the rate of starch hydrolysis, starch can be classified as rapidly digested starch (RDS), slowly digested starch (SDS), and resistant starch (RS) (Englyst et al., 1992). RDS is detrimental to health due to the rapid rate of digestion and absorption, which can lead to a range of metabolic disorders, such as rapidly rising blood glucose after meals, insulin resistance, and obesity (Alatrach et al., 2019; Zheng et al., 2020). Conversely, SDS and RS help to maintain glycaemic stability and increase satiety, potentially reducing the risk of obesity and type II diabetes (Gao et al., 2024). Regarding starchy staple foods, they constitute the source of intake for almost half of the world's population (Yi & Li, 2022). However, the intake of such refined starches often leads to the above health problems. Therefore, how to slow down the digestion of starch and increase the SDS or RS content has become a hot topic in current research in food science and nutrition.

Currently, research and development on starches with slow digestibility mainly focus on improving RS content through physical, chemical, or enzymatic modifications. Among them, resistant starch type 5 (RS5) has attracted much attention due to its ability to inhibit the swelling of starch granules and reduce the rate of starch digestion. As the RS5 type starch-polyphenol complex, recently more popular in research, where the guest molecule (polyphenol) binds to starch by occupying the hydrophobic helical structural domains in starch to form a tighter structure, thus effectively slowing down starch hydrolysis (Bharati et al., 2019; Sun & Miao, 2020). This mode of interaction, which includes CH-π interactions and hydrogen bonding interactions of α-1,4 glycosidic bonds, can significantly increase the RS content (Amoako & Awika, 2019; Liu et al., 2019).

In general, the conventional methods in preparing starch-polyphenol complexes usually involve the use of chemicals, high temperatures, or

* Corresponding authors.
E-mail addresses: duyiqun@ahau.edu.cn (Y. Du), yuzhenyuHF@163.com (Z. Yu).

https://doi.org/10.1016/j.fochx.2024.101919
Received 7 July 2024; Received in revised form 17 October 2024; Accepted 21 October 2024
Available online 22 October 2024

adjustment of pH, which may inadvertently compromise the quality and stability of these complexes (Raza et al., 2024). In addition, the traditional preparation of starch-polyphenol complexes by conduction heating produces relatively small amounts of V-type complexes, which are predominantly non-inclusion complexes (Lorentz et al., 2012). On the other hand, there is a growing interest in exploring alternative chemical or thermomechanical techniques that can enhance the yield of starch-polyphenol complexes while maintaining their structural integrity. Among these methods, ball milling pretreatment has attracted much attention due to their ability to induce structural changes in starch and polyphenols in food systems. It is a new method of applying friction, shear, collision, impact and various other mechanical forces to change the microstructure of solid particles, which is valued by the food industry for its environmentally friendly properties (Wang et al., 2021), efficient and low-cost features. It has been shown that the mechanical forces of ball milling can alter the structure and properties of starch (Kerr et al., 2001). Furthermore, the improvement of the starch structure by ball milling pretreatment supports the ability to form complexes with other guest molecules, resulting in more stable V-type complexes.

Ferulic acid (FA) is a hydroxycinnamic acid widely found in many fruits and vegetables and is sometimes referred to as a “chain-breaking” antioxidant because of its free radical scavenging properties (Kumar & Pruthi, 2014; Mancuso & Santangelo, 2014). Recently, research on FA has indicated that it has good pharmacological effects and biological activities such as antioxidants and anticancers in humans (Paiva et al., 2013). In addition, it has been shown that FA reduced the rate of starch hydrolysis by altering the secondary structure of digestive enzymes (Zheng et al., 2020). At the same time, it has been found that polyphenols not only can form complexes with starch molecules and enhance their structural density, but also inhibit the activity of digestive enzymes, thus slowing down the process of starch digestion (Karunaratne & Zhu, 2016). The use of starch-polyphenol complexes not only improves quality characteristics but also product acceptance. Although the interaction of starch with some polyphenols affecting the physicochemical properties of their complexes has been studied, few studies have been reported on the formation and properties of pretreated starch-polyphenol complexes.

Therefore, this study aimed to explore the formation mechanism, multi-scale structure and digestibility of ball milling pretreated modified HACS-FA complexes, and to elucidate their mechanism of action through density functional theory (DFT) calculations. Specifically, we performed scanning electron microscopy, X-ray diffraction, Raman spectroscopy, and Fourier transform infrared spectroscopy to analyze the micromorphology, crystalline structure, and chemical bonding of the high amylose corn starch (HACS)-ferulic acid (FA) complexes. The findings of this study are expected to provide an important reference and theory for the development and application of starch-polyphenol complexes and to promote the development of highly efficient resistant starch (e.g. RS5) and its application in food science and nutrition.

2. Materials and methods

2.1. Materials

High amylose corn starch with a 70 % amylose content was sourced from Quanyinxiangyu Biotechnology Co., Ltd. (Beijing, China). Ferulic acid with a purity of 99 % (CAS: 1135-24-6) was supplied by Aladdin Co., Ltd. (Shanghai, China). α-amylase (CAS: 9000-90-2, ≥5 U/mg, from porcine pancreas) was provided by Yuanye Biotechnology Co., Ltd. (Shanghai, China). Amyloglucosidase (EC 3.2.1.3, 260 U/mL, from aspergillus niger) was purchased from Sigma-Aldrich Chemical Co. (St. Louis, MO, USA). All other reagents used in this study were procured from Sinopharm Chemical Reagent Co., Ltd. (Shanghai, China) and these reagents were of analytical grade.

2.2. Preparation of ball milling pretreated modified starch-polyphenol complexes

2.2.1. Preparation of ball milling pretreated modified starch

50 g of HACS was modified using a ball mill (YD-YXQM-4 L, Changsha, China) with a rotation speed of 500 r/min and 10 min alternating rotation. The treatment times were 20, 40, 60, 120 and 180 min. In addition, the ball milling temperature was maintained at −18 to −10 °C using liquid nitrogen. The prepared samples were named HACS-”X". The “X” represented the treatment time.

2.2.2. Preparation of ball milling pretreated modified HACS-FA complexes

10 g (10 %, *w/v*) of HACS with the above different treatment times was accurately weighed and dispersed in deionized water and gelatinized for 1 h at 130 °C in a high-pressure steam sterilizer (LDZX-50 KB, Shanghai ShenAn Medical, Shanghai, China). Then, after adding 1 g of FA dissolved in ethanol to the starch paste, keep stirring for 1 h at 95 °C. Finally, the preparation was washed 2–3 times using 50 % alcohol and centrifuged for 10 min at 5000 rpm. The precipitate was dried at 40 °C overnight. The prepared samples were named HACS-”X"-FA and “X” was the ball milling time.

2.3. Determination of amylose content

Slightly modified according to the method of Chan et al. (2021). Add 100 mg of sample, 1 mL of 95 % ethanol, and 9.0 mL of 1.0 mol/L NaOH solution to a conical flask, shake well, and place for 10 min in a 100 °C water bath. 5.0 mL of the above solution was cooled to room temperature, 1.0 mL of CH_3COOH solution and 2.0 mL of iodine solution (solution of 0.2 % I_2 and 2.0 % KI) were added and water was added to 100 mL. The optical density at 620 nm was determined by a microplate reader (VICTOR Nivo, PerkinElmer, U.S.A.)

2.4. Cold water solubility and selling power

Slightly modified based on the method of Wang et al. (2016). Specific details were provided in the Supplementary material. The cold water solubility and swelling power were calculated according to the following equations.

$$\text{Cold water solubility (\%)} = \frac{w_1}{w_0} \times 100$$

$$\text{Swelling power (\%)} = \frac{w_3}{w_0 \times (100 - \textit{Cold water solubility})} \times 100$$

among them, W_1 is the quality of the supernatant liquid after drying, W_0 is the quality of the starch, and W_3 is the quality of the precipitate.

2.5. Fourier transform infrared spectroscopy (FTIR)

FTIR spectra was obtained using an FTIR spectrometer (Nicolet IS50, Thermo Fisher, USA). The spectra was scanned from 4000 to 400 cm^{-1} at a resolution of 4 cm^{-1}. Samples were diluted with anhydrous KBr and pressed into thin sheets. The deconvoluted spectra was used to calculate the absorbance ratio of 1047/1022 cm^{-1} using Omnic software (Li et al., 2024).

2.6. X-ray diffraction (XRD)

XRD patterns of samples were obtained using an X-ray diffractometer (TTR-III; Rigaku Company. Ltd., Tokyo, Japan) operated at 40 kV. The scan range was 5–40° at a rate of 5°/min with a step size of 0.02°. The relative crystallinity (RC) was analyzed using MDI Jade 6.0 software with the following equation:

$$RC\ (\%) = A_c/(A_c + A_a) \times 100\%$$

where A_c and A_a were the total areas of the crystalline and amorphous peaks, respectively, in the XRD patterns.

2.7. Gel permeation chromatography (GPC)

The molecular weight of samples was determined by GPC. Firstly, the samples were dissolved in a suitable solvent and filtered through a 0.45 μm filter membrane to remove insoluble impurities. Then, the samples were injected into a GPC system (Waters, USA) and separated using a gel column (Waters Ultrahydrogel 250). The detection was performed using a multi-angle laser light scattering detector (MALS) and an oscillometric refractive detector (RI). The GPC results were manipulated using ASTRA software.

2.8. Determination of FA content of the complexes

100 mg (dry basis) of the complex was dissolved in 5.0 mL of DMSO and then centrifuged at 4000 ×*g* for 10 min. Then, the polyphenol content was determined by the forintol method. Briefly, 0.5 mL of the solution was mixed with 1.5 mL of deionized water, 1.0 mL of forintol reagent was added and mixed well and the reaction was carried out for 10 min, then 1.0 mL of 8 % (*w*/w) Na_2CO_3 solution was added to it and kept in darkness at room temperature for 3 h. The absorbance of the solution at 760 nm was measured by a microplate reader (VICTOR Nivo, PerkinElmer, U.S.A.)

2.9. Scanning electron microscope (SEM) of HACS-FA complex

The microscopic morphology of all samples was observed by SEM (S-4800, Hitachi, Tokyo, Japan). The samples were mounted on conductive adhesive and plated with gold, then examined at an accelerating voltage of 3 kV (Liu et al., 2024).

2.10. Raman spectroscopy of HACS-FA complex

To characterize the short-range ordering of HACS and HACS-FA complexes, we performed measurements using Raman spectroscopy (LabRAM HR Evolution, Horiba/Jobin Yvon, France). The half peak width at 480 cm^{-1} was obtained by using Peakfit software. In addition, the test range was 3200–100 cm^{-1} and the laser source was 785 nm.

2.11. ^{13}C nuclear magnetic resonance (NMR) spectroscopy

200–300 mg of starch samples were placed in a rotating cylinder of 4 mm diameter and recorded with a spectrometer (AVANCE III 500, Bruker Ltd., Karlsruhe, Germany). The number of scans was 3000 and the interval between cycles was 2 s. The obtained spectra were processed using the method of Tan et al. (2007).

2.12. ^{1}H nuclear magnetic resonance (NMR) spectroscopy

An adequate quantity of the sample was dissolved in deuterated dimethylsulfoxide, and spectral data were obtained using an Agilent DD2–600 MHz spectrometer (Agilent Technologies, USA) at 500 MHz, 25 °C, with a pulse angle of 30°, a delay of 10 s, and an acquisition time of 2 s. The relative contents of the α-1,4- and α-1,6-glycosidic bonds were obtained by dividing the corresponding peak areas (5.11 and 4.94 ppm, respectively) by the combined area of the peaks of both moieties (Zhong et al., 2022). The degree of branching (DB) of starch was obtained according to the following equation:

$$DB\ (\%) = \frac{I\alpha - 1,6}{I\alpha - 1,6 + I\alpha - 1,4} \times 100$$

where Iα-1,6 represents the relative area of the α-1,6 glycosidic bond; Iα-1,4 represents the relative area of the α-1,4 glycosidic bond.

2.13. In vitro digestion

The method of Englyst et al. (Englyst et al., 1992) was optimized for the determination of RDS, SDS, and RS in starch. 0.2 g (dry basis) of the starch sample was taken in a conical flask, 20 mL of 0.1 mol/L sodium acetate buffer (pH 5.2) was added, and the mixture was boiled for 30 min. The mixture was then cooled to about 37 °C, 5 mL of enzyme solution (α-amylase: 5 U/mg and glucosidase:260 U/mL), and placed in a water bath shaker (37 °C, 170 stoke/min). After 20 min, 0.5 mL of the mixture was taken and added to 20 mL of 70 % ethanol, then centrifuged for 5 min (4000 r/min). Add 0.1 mL of the supernatant to 3 mL of GOPOD solution (Nanjing Jianjian Institute of Bioengineering, Nanjing, China) and incubate at 37 °C in a water bath for 10 min. Finally, the absorbance was measured at 505 nm. After 120 min, the absorbance of the sample was measured in the same way as above. The calculation was as follows:

$$RDS\ (\%) = [(G_{20} - G_0) \times 0.9]/TS \times 100$$

$$SDS\ (\%) = [(G_{120} - G_{20}) \times 0.9]/TS \times 100$$

$$RS\ (\%) = (1 - RDS - SDS) \times 100$$

where 0.9 was the transformation coefficient from starch to glucose, and G_{20} and G_{120} represented the glucose contents at 20 and 120 min, respectively. *TS* was the mass of the total starch dry base (mg).

2.14. Computational details

We used the PubChem website to download the 3D structure of FA. Since starch has a huge molecular weight as well as a multi-scale structure, it is difficult to simulate the whole starch structure by DFT calculations. Therefore, we selected a starch molecule fragment (DP = 10) of the starch model as the calculation model. The base group B3LYP/6-311G^{++} used to optimize the molecular structure of starch with FA was initiated by GaussView 6.0.16 and the analysis was implemented by Gaussian output files. The electrostatic potential was then plotted using Multiwfn (Lu & Chen, 2012) in combination with VMD. After that, 50 dockings of the HACS-FA complex were simulated using the AutoDock program, and the structure with the smallest binding energy was selected as the docking model, and the binding process was visualized and analyzed using PyMol software (http://www.pymol.org/). At the same time, the interaction between the both was further analyzed in the Multiwfn program.

2.15. Statistical analysis

All numerical results are the average of at least three independent replicates. Analysis of variance using Duncan's test. Values in the same column with different superscripts are significantly different ($p < 0.05$).

3. Results and discussion

3.1. Amylose content analysis

From Fig. 1A, the natural HACS had an amylose content of 71.44 %. As the ball milling time increased, the content of amylose increased significantly to 79.29 %. This was primarily associated with the change of the original structure of starch granules under mechanical force. On the one hand, the α-1,6 glycosidic bond was broken under the shear and extrusion of ball milling, and amylopectin was stripped of the side chains to produce short amylose starch (Hao et al., 2024). On the other hand, the α-1,4 glycosidic bond of amylose was similarly broken under the conditions of ball milling pre-treatment modification, and the long chain of starch was cleaved into many linear short chains. As a result, the amylose content of HACS increased significantly, depending on the

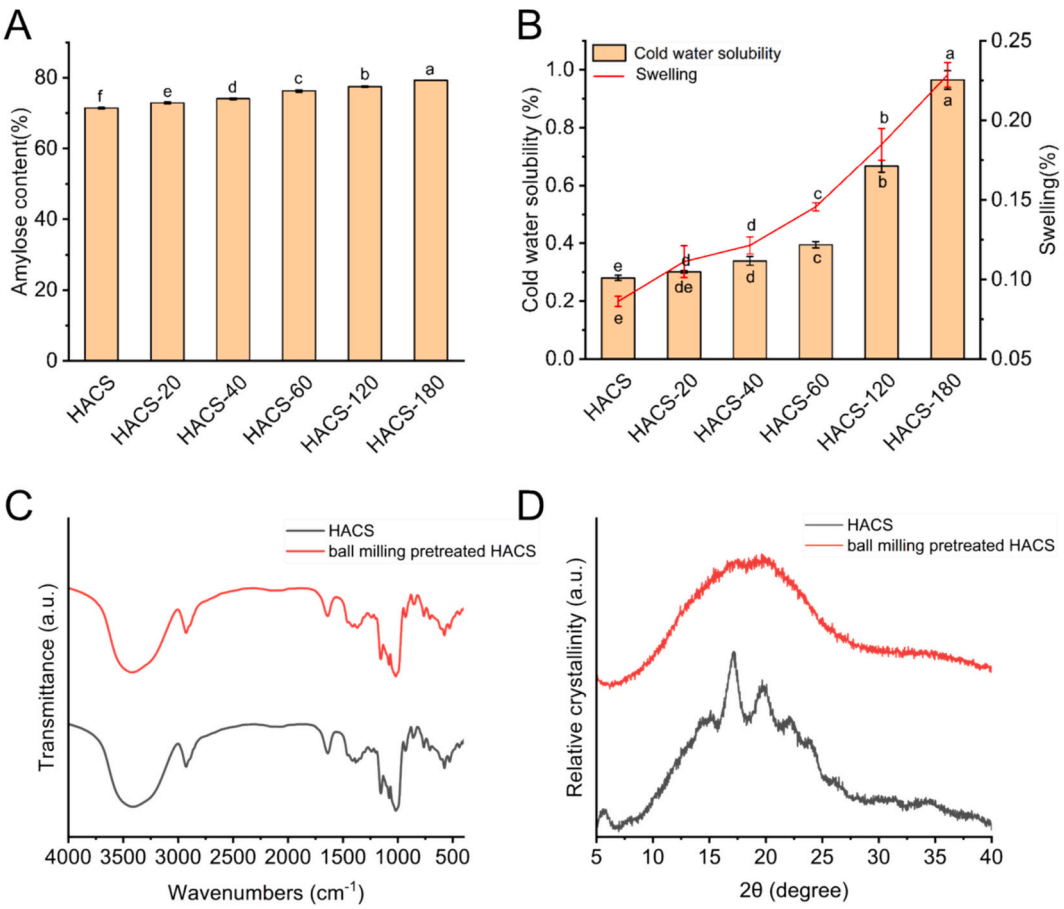

Fig. 1. The amylose content (A), cold water solubility and swelling (B), XRD (C) and FT-IR (D) for HACS treated with different ball milling times. All the values are the mean ± standard deviations. The mean values with different superscripts in a column indicate significant differences ($P < 0.05$).

duration of the ball milling treatment.

3.2. Water solubility and swelling power analysis

A significant increase in the cold water solubility and swelling of HACS was found in Fig. 1B, where the cold water solubility increased from 0.28 % to 0.96 % as well as the swelling power improved from 0.08 % to 0.23 % after 180 min. This would be because ball milling caused damage to the starch structure, and a large number of cracks appeared on the surface of the granules. In this case, water molecules could more easily penetrate the starch granules, and inter and intramolecular hydrogen bonding of starch molecules could maintain the water entering the starch granules, resulting in increased starch solubility and swelling. On the other hand, ball milling gradually changed the semi-crystalline to an amorphous state and reduced the content of double helix in amylose, thus promoting the increase of starch solubility and swelling.

3.3. Molecular structure analysis

The FTIR spectra of HACS treated with different ball milling times is shown in Fig. 1C. By comparing the individual spectra, there was no obvious change in the individual absorption peaks, and none of the peaks were generated, indicating that ball milling modification caused no new chemical bond or functional group formation in the starch molecules. In addition, in the deconvolution analysis (Fig. S1A), we found that the $R_{1047/1022}$ of ball milling pretreated HACS decreased from 0.783 to 0.712 ($p < 0.05$), indicating that the short-range ordering of starch molecules was disrupted, changing the structure of the HACS molecules, which laid the foundation for the complexation with FA. The above results indicated that the ball milling pretreatment modified starch belonged to a kind of physical modification, and would not introduce new groups to be generated. Liu et al. (2021) who used ball milling to treat different types of glutinous rice starch also gave the same results.

3.4. Crystal structure analysis

Fig. 1D shows the XRD patterns of HACS pretreated by ball milling at different times. The structure of HACS was typical of B-type starch, with intense diffraction peaks appearing around 2θ of 17° and 19°, and smaller diffraction peaks appearing around 2θ of 5.6°, 15°, 22° and 24° (No & Shin, 2023). With the increasing treatment time, the diffraction peaks gradually disappeared, indicating that the mechanical force of ball milling destroyed the original arrangement between the molecular chains of starch, weakened the intra- and intermolecular hydrogen bonding interactions, resulting in the disorderly arrangement of the molecular chains of starch (Lu et al., 2018). The changes of starch from crystalline structure to amorphous state and the breakage of intermolecular glycosidic bonds of starch ultimately resulted in the breakdown of the starch crystal structure (Hao et al., 2023), which also indicated the success of the preparation of ball milling pretreated starch, which will be used for subsequent experiments.

3.5. Molecular weight analysis

The impact of the modification of the HACS molecular weight by the ball milling pretreatment was analyzed using GPC, and the findings are

presented in Fig. 2. Native HACS had a weight average molecular weight (Mw) of 199.905 kDa. As the processing time increased, the molecular weight gradually decreased. When the time reached 180 min, the molecular weight of HACS decreased to 92.155 kDa, indicating that amylose and amylopectin were broken down during the pre-treatment modification process. The starch molecule was mainly formed by a long chain molecular structure of glucose units linked by α-1,4- and α-1,6-glycosidic bonds. These glycosidic bonds were easily broken by mechanical forces during ball milling pretreatment, especially the relatively weak α-1,6-glycosidic bonds were more susceptible, which led to the degradation of starch macromolecules into smaller molecular fragments (Cavallini & Franco, 2010). In addition, the ball milling treatment may also lead to the disruption of hydrogen bonds between starch molecules, further affecting the molecular structure stability of starch. The destruction of hydrogen bonds made starch molecular chains more susceptible to breakage by external forces, thus accelerating the reduction of molecular weight.

3.6. FA content analysis

Table 1 shows the FA content in the HACS complexes. From the table, it showed that the FA content in the HACS-FA complexes increased as the ball milling treatment time increased. The value of FA increased

Table 1
The FA content in HACS-FA complexes treated with different ball milling times.

Sample	FA content (mg/g)
HACS-20-FA	18.33 ± 0.15^{e}
HACS-40-FA	21.62 ± 0.60^{d}
HACS-60-FA	23.61 ± 0.28^{c}
HACS-120-FA	25.71 ± 0.35^{b}
HACS-180-FA	28.96 ± 0.61^{a}

All the values are the mean ± standard deviations. The mean values with different superscripts in a column indicate significant differences ($P < 0.05$).

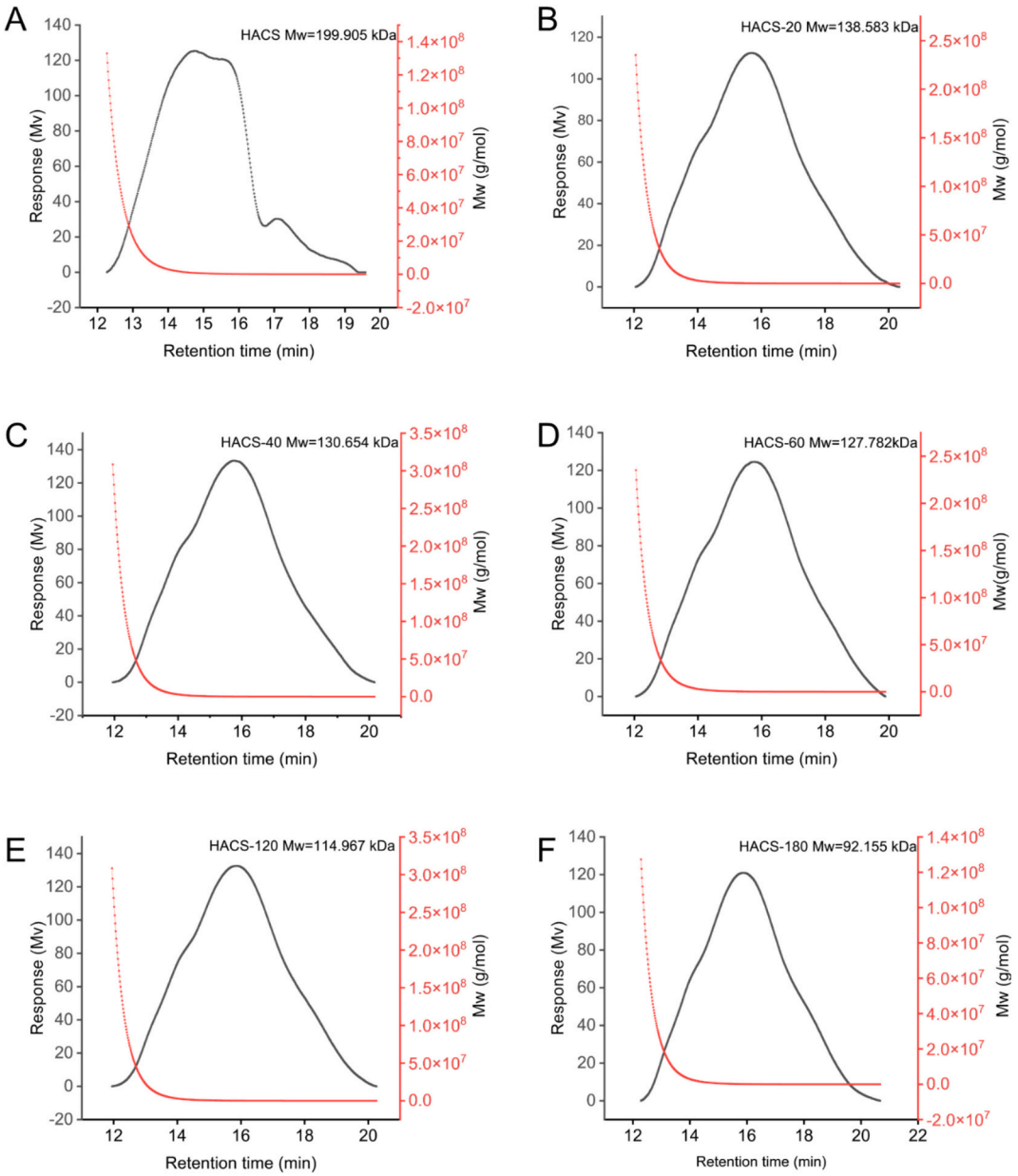

Fig. 2. Effect of ball milling on molecular weight distribution of high amylose corn starch.

from 18.33 mg/g to 28.96 mg/g after 180 min of treatment. We speculated that starch with longer ball milling times could capture more FA. This was achieved by disrupting the structure of the double helix within the starch molecules during the pre-milling process, causing the double helix to disintegrate. FA was more readily accessible to the hydrophobic cavity of the HACS through non-covalent interactions, which resulted in a remarkable increase of the polyphenol content in the complex as the duration of the ball milling treatment increased. We found that HACS-FA complex formation is promoted by ball milling pretreatment modification.

3.7. SEM analysis

The SEM of the FA, HACS, and HACS-FA complexes is shown in Fig. 3. The surface of FA in the crystalline state was relatively rough and irregularly stick-shaped, and HACS was elliptical or irregularly shaped with a smooth surface. The HACS-FA complex was in the form of lumps of varying sizes, and there were obvious cracks and grooves between the starch granules. This was attributed to the fact that the surface of the starch granules was cracked and grooved by the ball milling process, and during the complexing process, the granular structure of the starch was disrupted, forming plenty of short-chain linear amylose, which aggregated and reformed into double helices during short-term retrogradation (Van Hung et al., 2012). Moreover, the surface of the complex granules was smooth after adding FA. This may be due to the fact that FA may be trapped in the hydrophobic core of the double helix formed between linear amylose molecules, thereby making the amorphous and semi-crystalline regions more structured and dense (Maibam et al., 2023).

3.8. XRD analysis

The XRD patterns of the HACS and ball milling pretreated modified HACS-FA complexes are presented in Fig. 4A. The native HACS had intense diffraction peaks around 15°, 17°, 18° and 23.5°, indicating that HACS belonged to type B starch, and the complexes showed intense diffraction peaks at 13°, 17° and 20°, which shows a V-type crystal structure (Hao et al., 2023). In Table 2, the relative crystallinity of the HACS-FA complexes increased with the milling time, increasing from 22.52 % to 32.76 % after 180 min of milling. This suggested that HACS and FA formed more ordered crystals through hydrogen bonding. This was mainly achieved by destroying the crystalline regions of the starch molecules, resulting in starch being more susceptible to interactions with other guest molecules. On the one hand, the addition of pretreatment would cause the starch to produce short amylose starches. Short amylose starches were easily orientated in solution, easily regenerated, and therefore easy to bind to FA (Tian & Sun, 2020). On the other hand, ball milling treatment made FA more accessible to the hydrophobic cavity of starch. The hydroxyl groups of polyphenols could bind to the starch chains, thus enhancing the long-range ordering of the starch molecules and making the crystalline regions more compact (Li et al., 2021).

3.9. FITR and Raman spectroscopy analysis

The FTIR spectra of the HACS and ball milling pretreated modified HACS-FA complexes is presented in Fig. 4B. The broad peak at 3385 cm^{-1} in the FTIR of HACS was attributed to the intermolecular -OH stretching vibration, and the absorption peak at 2929 cm^{-1} was attributed to the anti-symmetric stretching vibration of methylene (-CH_2). Comparing the spectra of native HACS and HACS-FA complexes at various processing times, we found that the HACS-FA complex showed an additional peak at 1506 cm^{-1} (Fig. 4D), which could be attributed to the C═C stretching vibration in the molecular structure of FA. In this case, a peak at 1640 cm^{-1} was associated with the absorption of water in the amorphous region of starch, where the FA molecules would enter the hydrophobic cavity of the starch, exposing more polar groups to the hydrophobic cavity, resulting in a weakening of the absorption peaks. At 1047 and 1022 cm^{-1}, which are sensitive to the ordered and amorphous structures of starch, respectively, the ratio of the absorbance at 1047/1022 cm^{-1} ($R_{1047/1022}$) could be used to quantify the degree of starch ordering (Fig. 4C). In Table 2, $R_{1047/1022}$ showed a marked change from 0.804 to 0.983 with increasing milling time, demonstrating that milling treatment made FA more accessible to the hydrophobic cavities of the starch and that intramolecular and intermolecular hydrogen bonding between starch and polyphenols would lead to the formation of more tightly bonded complexes, which further indicated that ball-milling pretreatment induced a more compact and ordered structure.

The peak located at 480 cm^{-1} in Raman spectra is related to the vibration of the carbon skeleton, and the half peak width of this peak is affected by the crystal structure of starch, in which the smaller the value of the full width at half-maximum (FWHM), the higher the short-range ordering of the starch molecular structure (Wang et al., 2017). Fig. 5A

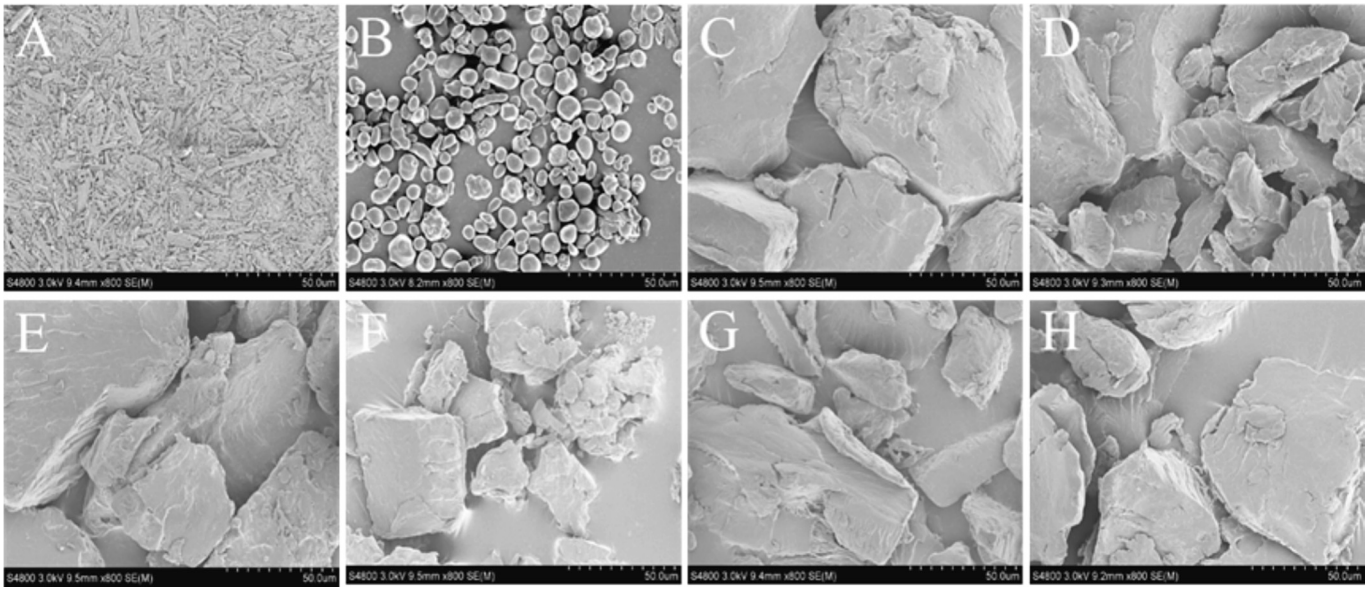

Fig. 3. SEM images of FA, Native HACS and HACS-FA complexes treated with different ball milling times. (A: FA, B: HACS, C: HACS-FA, D: HACS-FA-20, E: HACS-FA-40, F: HACS-FA-60, G: HACS-FA-120, H: HACS-FA-180. The magnification of A-H is 800×.).

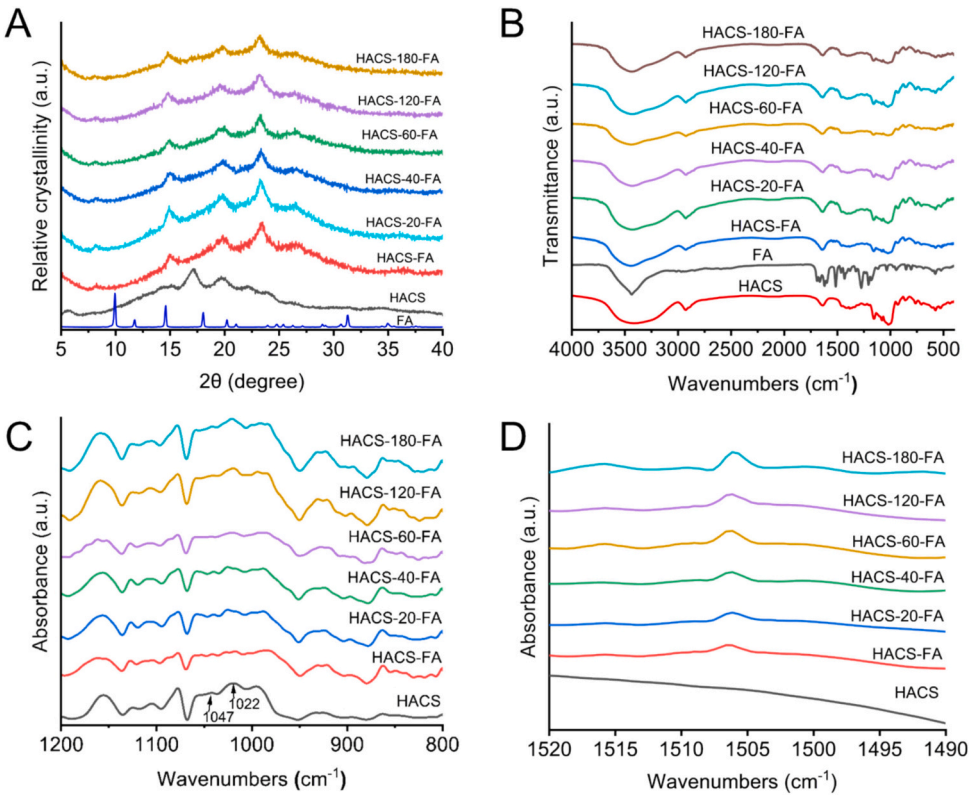

Fig. 4. The X-ray diffraction patterns (A), FT-IR spectra (B), deconvoluted FT-IR spectraand (C) and localised FT-IR spectra (D) for HACS and HACS-FA complexes treated with different ball milling times.

Table 2
XRD, FT-IR, FWHM and In vitro digestibility of HACS and ball milling pretreated modified HACS-FA complexes.

Sample	Crystallinity (%)	$R_{1047/1022}$	FWHM at 480 cm^{-1}	RDS	SDS	RS
HACS	21.02 ± 0.86^{f}	0.729 ± 0.00^{e}	26.594 ± 0.07^{a}	45.56 ± 0.58^{a}	15.70 ± 0.84^{d}	38.74 ± 1.41^{e}
HACS-FA	22.52 ± 0.44^{f}	0.804 ± 0.00^{d}	19.160 ± 0.60^{b}	40.65 ± 1.41^{b}	18.12 ± 0.61^{cd}	41.23 ± 1.74^{de}
HACS-20-FA	24.58 ± 0.09^{e}	0.834 ± 0.00^{cd}	17.997 ± 0.29^{c}	37.70 ± 0.81^{b}	19.53 ± 0.83^{c}	42.77 ± 1.51^{d}
HACS-40-FA	26.25 ± 0.11^{d}	0.845 ± 0.01^{cd}	16.369 ± 0.66^{d}	32.04 ± 0.81^{c}	23.57 ± 0.89^{ab}	44.39 ± 1.26^{d}
HACS-60-FA	27.81 ± 0.22^{c}	0.869 ± 0.01^{bc}	15.525 ± 0.33^{e}	27.40 ± 1.31^{d}	22.36 ± 0.96^{b}	49.56 ± 0.90^{c}
HACS-120-FA	30.49 ± 0.38^{b}	0.905 ± 0.02^{b}	14.868 ± 0.02^{e}	19.70 ± 1.76^{e}	25.29 ± 1.34^{a}	55.31 ± 1.33^{b}
HACS-180-FA	32.76 ± 0.76^{a}	0.983 ± 0.02^{a}	13.461 ± 0.20^{f}	16.13 ± 0.97^{f}	22.73 ± 1.00^{ab}	61.13 ± 0.62^{a}

Means ± standard deviations of repeated trials are given, and different lowercase letters in the same column with significant differences ($P < 0.05$). RDS, rapidly digestible starch (%); SDS, slowly digestible starch (%); RS, resistance starch (%).

shows the Raman spectra of natural HACS and HACS-FA complexes. It has been shown that the FWHM value of the 480 cm^{-1} peak in spectra can be used to calculate the short-range ordering of starch (Maibam et al., 2023). The FWHM of HACS-FA complexes decreased noticeably from 19.1599 to 13.4607 after 180 min (Table 2), indicating that HACS-FA complexes greatly improved short-range ordering. This was caused by the huge number of short amylose molecules produced during the ball milling process, which self-assembled to form a better-ordered helical structure. Meanwhile, through hydrophobic interaction, FA formed a denser and more ordered complex with HACS. We found that new diffraction peaks appeared at 1604 and 1630 cm^{-1} for the HACS-FA complexes compared to HACS, corresponding to the stretching vibrations of the aromatic ring and C═C side chain in FA, respectively (Chi et al., 2019). In addition, there was a positive correlation between the duration of the treatment, the amount of FA in the complexes, and the intensity of the diffraction peaks, which further confirmed that ball milling treatment could promote the formation of HACS-FA complexes (Liu et al., 2021). A previous study also indicated that the intensity of the bimodal peaks in the same band increased with increasing phenolic acid substitution (Lu et al., 2023).

3.10. ^{13}C CP/MAS NMR spectra analysis

Fig. 5B shows the NMR spectra of HACS and ball milling pretreated modified HACS-FA complexes. The characteristic peak of C1 region was located at 98–105 ppm, and the resonances at 68–78 ppm were ascribed to C2, C3, and C5 sites, and resonances at 77–86 ppm and 58–65 ppm corresponding to C4 and C6 sites, respectively. Of which C1 and C4 were suggested to be sensitive to the helical structural alternation of starch (Hao et al., 2023). After ball milling pretreatment, the typical peaks of starch (C1, 2, 3, 5) did not change significantly, while new peaks at around 31 ppm were observed, which became more obvious with increasing pretreatment time. This indicated that the starch-polyphenol complex was characterized by a typical V-type structure. In order to investigate the content of the helical structure and amorphous region of HACS and ball milling pretreated HACS-FA complexes, the ^{13}C CP/MAS NMR spectra were solved to calculate the correlation area to obtain the

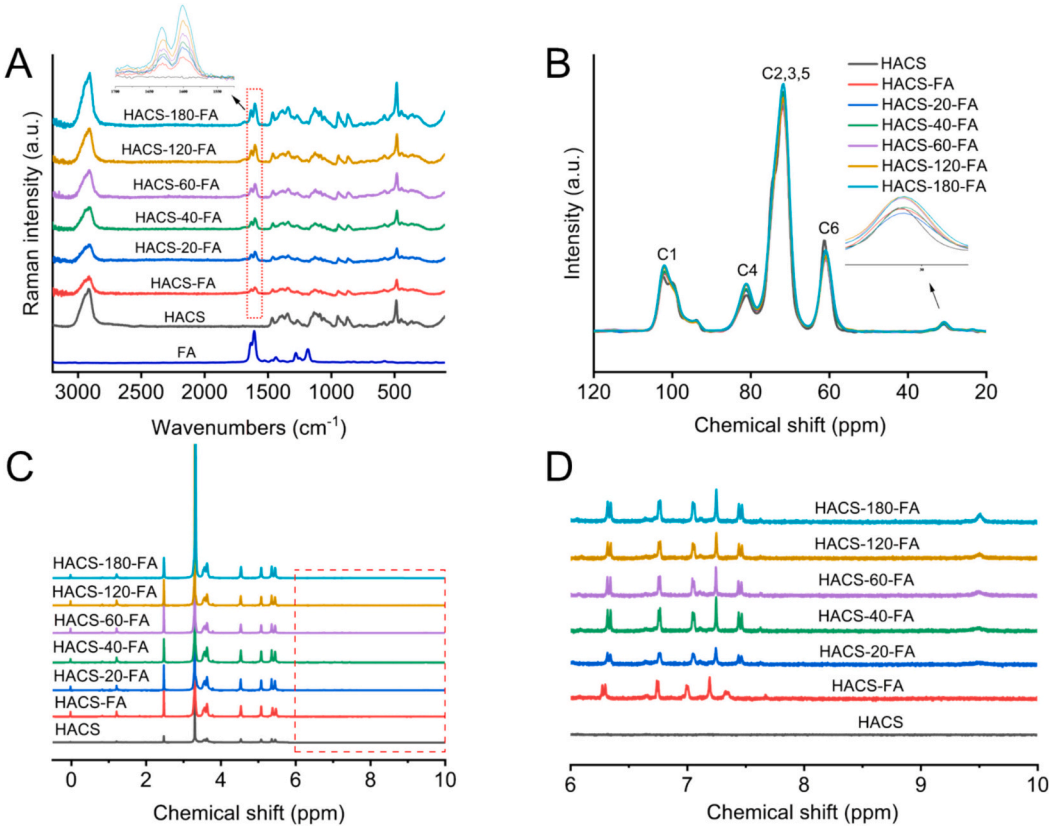

Fig. 5. The Raman spectra (A), ^{13}C NMR CP/MAS spectra (B) and hydrogen nuclear magnetic resonance spectra (C—D) for HACS and HACS-FA complexes treated with different ball milling times.

content of double helical structure, single helical structure, and amorphous region (Brewer et al., 2012). Changes in the amorphous and helical structures of these samples are shown in Table S1. Under ball milling pretreatment conditions (increasing treatment time), the addition of FA resulted in a slight increase in the content of single and double helices formed due to complexation, with a tendency for the amorphous region to show a decrease ($p < 0.05$). FA may enter the cavities of amylose or long side chains of amylopectin to form starch-polyphenol complexes with single helical structure (Li et al., 2022). At the same time, ball milling pretreatment disrupted the glycosidic bonds in starch and increased the proportion of amylose, thus allowing more FA to enter the hydrophobic cavities of these chains to form single helical structure (He et al., 2020). On the other hand, the ball milling process shortened the starch chains and promoted the formation of hydrogen bonds between FA and HACS, contributing to the formation of the double helix structure (Zheng et al., 2021). This resulted in a more ordered and dense HACS-FA complex, which was also consistent with their corresponding the XRD.

3.11. ^{1}H NMR spectra analysis

The interaction between starch and polyphenols at the molecular level was analyzed using ^{1}H NMR spectroscopy. The ^{1}H NMR spectra for HACS and HACS-FA complexes are illustrated in Fig. 5C-D. Signal peaks corresponding to DMSO and water molecules were observed at 2.49 ppm and 3.33 ppm, respectively, across all samples. Proton signals for starch appeared at 5.49 ppm (3-OH), 5.40 ppm (2-OH), 5.11 ppm (1-H), and 4.57 ppm (6-OH). The proton signals detected in the range of 4.5–5.6 ppm were attributed to the isomeric and hydroxyl protons of starch monomers (Maibam et al., 2023). Additional signal peaks appeared in the NMR hydrogen spectra of the complexes compared to HACS, and the presence of a pair of vinyl proton signal peaks at 6.7 and 7.8 ppm confirmed the presence of FA molecules in the complexes. Aromatic protons in the structure of the FA molecule are observed in the range of 6.9–7.4 ppm, and the weak peak at 9.73 ppm was associated with phenolic hydroxyl groups in the structure of the FA molecule (Fang et al., 2020; Maibam et al., 2023), and the intensity of the signal peaks becomes more and more pronounced with increasing pretreatment time. In addition, ^{1}H NMR spectra were used to determine the ratio of α-1,6 and α-1,4 glycosidic bonds of HACS to determine the degree of branching in the molecular structure of starch (Li et al., 2023). As can be seen from Fig. S1B, DB gradually decreased with the increase of ball milling pretreatment time, from 1.96 % to 0.93 %, indicating that amylopectin linked by α-1,6 glycosidic bonds is more easily damaged than amylose linked by α-1,4 glycosidic bonds (Liu et al., 2019). In addition, the ball milling treatment may also lead to the breakage of the original long amylose into short amylose, consistent with the amylose content analysis described above. On this basis, the greater the degree of binding of FA and ball milling pretreated HACS.

3.12. In vitro digestibility

The content of RDS, SDS, and RS of HACS and HACS-FA complexes is shown in Table 2. The RDS, SDS and RS content of HACS were 45.56 %, 15.70 %, and 38.74 %, respectively. As we expected, the addition of FA significantly decreased the starch digestibility while increasing the content of RS. In addition, the addition of FA increased the crystallinity of HACS and enhanced the short-range ordering structure of the complexes, as can be seen from the XRD spectra. At the ball milling treatment time of 180 min, the RDS content of the complex decreased from 40.65 % to 16.13 %, while the RS content rose from 38.74 % to 61.13 %. This indicated that, on the one hand, the complex of starch and FA molecules resulted in a denser structure, which enhanced the resistance to enzymatic hydrolysis and slowed down the rate of starch hydrolysis

(Romero Hernández et al., 2022). On the other hand, the relevant paper suggested that FA in the complex led to conformational changes in the digestive enzymes, thus further inhibiting the starch digestibility, which was another important factor that would be further investigated in future work (Sun & Miao, 2020). It was shown that the starch-polyphenol complex was a novel resistant starch (RS5), in which polyphenols occupied the hydrophobic helical cavity of starch through CH-π and hydrogen bonding interactions and bound to starch to form a V-shaped complex. The structure of the complex was more dense, thus effectively slowing down the rate of starch hydrolysis and significantly increasing the RS content. In addition, it has been shown that FA decreased the rate of starch hydrolysis by inhibiting the activities of α-amylase and α-glucosidase (Zheng et al., 2020), leading to changes in the structure of digestive enzyme secondary proteins. The new finding that starch-gallate alkyl ester complexes similarly inhibit starch digestion was consistent with the analyses in this study (Gutierrez et al., 2020).

3.13. Correlation analysis

Pearson correlation analysis was used to analysis the correlation between multi-scale structure and digestive properties (Fig. S1C) The results showed that the RDS of the complex was negatively correlated with XRD ($P \leq 0.001$), $R_{1047/1022}$ ($P \leq 0.001$), single helix ($P \leq 0.001$), and double helix ($P \leq 0.001$), and positively correlated with amorphous starch ($P \leq 0.001$) and FWHM ($P \leq 0.001$). The RS of the complex was positively correlated with XRD ($P \leq 0.001$), $R_{1047/1022}$ ($P \leq 0.001$), single helix ($P \leq 0.001$), and double helix ($P \leq 0.001$), and negatively correlated with amorphous starch ($P \leq 0.001$) and FWHM ($P \leq 0.001$). This indicated that the HACS-FA complexes pretreated by ball milling

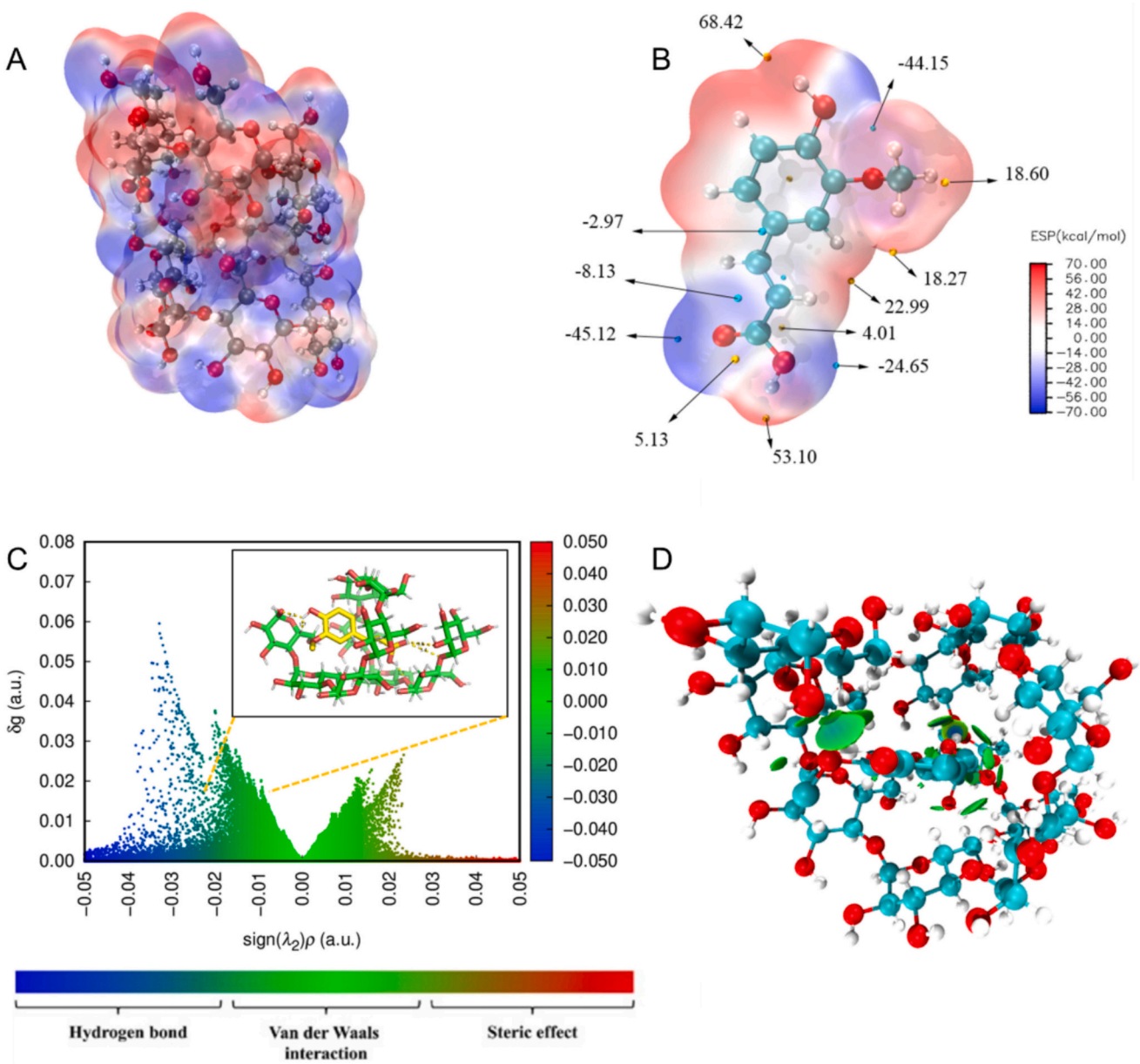

Fig. 6. The distribution of electrostatic potential (ESP) on the molecular surface of starch (DP = 10) (A) and ferulic acid (B); the red spheres represent oxygen atoms, cyan spheres represent carbon atoms and white spheres represent hydrogen atoms in the molecular structure. The RDG scatter (C) and the distribution of non-covalent interactions in real space (D) for the HACS-FA complex system; Where the red spheres represent oxygen atoms, the cyan spheres represent carbon atoms, and the white spheres represent hydrogen atoms. (For interpretation of the references to colour in this figure legend, the reader is referred to the web version of this article.)

had a higher content of long-range ordering structure and helical structure, which helped to slow down the digestion rate. Pearson correlation analysis showed that long−/short-range ordering, helical conformation, and fine structure affected the physicochemical properties and in vitro digestibility of the HACS-FA complexes.

3.14. DFT calculation analysis

To further understand the interaction mechanisms between HACS-FA complexes and elucidate the molecular basis of their structural alterations and digestive behavior, we performed DFT calculations and IGM analysis (Zhang et al., 2023). The ESP distributions for the HACS (DP = 10) and FA are depicted in Fig. 6A-B. The ESP distribution of free monomers in the figure can be visualized by the scale, i.e., the darker the blue colour represents a significant increase in the electron cloud density and the more negative charges in the corresponding region, whereas the darker the red colour represents the lower the electron cloud density and the more positive charge here. Our findings showed that the highest and lowest ESP values were located near the hydroxyl and carboxyl groups of HACS and FA (Zheng et al., 2022), suggesting these regions were key sites for molecular interactions. Molecular docking (Fig. 6C) showed the stabilization of FA molecules bound to HACS by hydrogen bonding. The results of IGM (Fig. 6C) analysis further showed that starch molecules appeared as thin and wide isosurfaces with FA molecules, indicating the mode of interaction between them. The green region indicated the presence of van der Waals forces and the blue region (Qiu et al., 2023) indicated the presence of a partial hydrogen bonding link between starch and FA. It could be seen that non-covalent interactions such as hydrogen bonding (confirmed by FTIR spectroscopy), van der Waals forces, and spatial steric drag effects were present in the complex system (Hao et al., 2024). In addition, FA entered the hydrophobic cavity of starch through hydrophobic interactions and formed a single helix complex, promoting the formation of the internal helical structure of starch, which was not a negligible factor. The specific HACS and FA complex systems non-covalent interactions in real space are shown in Fig. 6D. The hydrogen bonding between them (green plot) was mainly distributed between the hydroxyl, carboxyl of THE and starch molecules, which following the results of the above ESP analysis of the main interaction sites for the stable structure of this complex systems.

4. Conclusion

In this study, the formation mechanism, physicochemical properties, and the relationship between the multi-scale structure and digestive properties of ball milling pretreated HACS-FA complexes were investigated, and elucidated the intermolecular interactions by DFT calculations. The results showed that the amylose content of HACS was significantly increased ($p < 0.05$) and the average molecular weight was reduced to 92.155 kDa at the modification time of ball milling pretreatment from 0 to 180 min, which laid the foundation for the subsequent experiments. The FA content in the ball milling pretreated HACS-FA complex increased from 18.33 mg/g to 28.96 mg/g, and the degree of complexation was improved. The SEM results showed that the morphology of the complexes changed to irregular lumps. In addition, the crystallinity of the HACS-FA complexes increased by 11.74 % with increasing time of ball milling pretreatment, and the short-range ordering increased significantly. Notably, the contents of single and double helices in HACS-FA-120 were 10.50 % and 27.90 %, respectively, which showed an increasing trend ($p < 0.05$), indicating that the ball milling pretreated HACS-FA complexes had a more compact V-type structure. In terms of digestibility, the RS of HACS-FA complexes increased by 22.39 %, and the presence of FA inhibited starch digestibility. DFT calculations further suggested that the intermolecular interactions between HACS and FA were mainly hydrophobic, hydrogen bonding, and van der Waals forces. This study is expected to provide a new method for the efficient preparation of HACS-FA complexes and provide some insights into the relationship between their multi-scale structure and digestibility.

CRediT authorship contribution statement

Zongwei Hao: Writing – original draft, Methodology, Investigation, Data curation, Conceptualization. **Shengjun Han:** Validation. **Zhongyun Zhao:** Visualization. **Zongjun Wu:** Writing – review & editing, Software. **Hui Xu:** Writing – review & editing, Software, Investigation. **Chao Li:** Writing – review & editing, Methodology. **Mingming Zheng:** Formal analysis. **Yibin Zhou:** Formal analysis. **Yiqun Du:** Supervision, Funding acquisition, Conceptualization. **Zhenyu Yu:** Supervision, Project administration, Funding acquisition, Conceptualization.

Declaration of competing interest

The authors declare that they have no known competing financial interests or personal relationships that could have appeared to influence the work reported in this paper.

Data availability

Data will be made available on request.

Acknowledgements

This work was supported by the National Natural Science Foundation of China (32172162), Anhui Agricultural University Foundation for Stability and Introduction of Talent (rc352008, rc352212), the Key Research and Development Program of Anhui Province (2023n06020038, 2023n06020039). the Scientific Research Projects for Universities in Anhui Province (2024AH050479) and the Opening Project of Key Laboratory of Oilseeds Processing, Ministry of Agriculture and Rural Affairs, China (202405). The authors would like to thank the Shiyanjia Lab (www.shiyanjia.com) for the assistance of XRD analysis.

Appendix A. Supplementary data

Supplementary data to this article can be found online at https://doi.org/10.1016/j.fochx.2024.101919.

References

Alatrach, M., Agyin, C., Mehta, R., Adams, J., DeFronzo, R. A., & Abdul-Ghani, M. (2019). Glucose-mediated glucose disposal at baseline insulin is impaired in IFG. *The Journal of Clinical Endocrinology & Metabolism, 104*, 163–171.

Amoako, D. B., & Awika, J. M. (2019). Resistant starch formation through intrahelical V-complexes between polymeric proanthocyanidins and amylose. *Food Chemistry, 285*, 326–333.

Bharati, S., Hardeep, S., & Gujral.. (2019). Influence of nutritional and antinutritional components on dough rheology and *in vitro* protein & starch digestibility of minor millets. *Food Chemistry, 299*, Article 125115.

Brewer, L. R., Cai, L., & Shi, Y. (2012). Mechanism and enzymatic contribution to in vitro test method of digestion for maize starches differing in amylose content. *Journal of Agricultural and Food Chemistry, 60*(17), 4379–4387.

Cavallini, C. M., & Franco, C. M. L. (2010). Effect of acid-ethanol treatment followed by ball milling on structural and physicochemical characteristics of cassava starch. *Starch - Stärke, 62*(5), 236–245.

Chan, C., Wu, R., & Shao, Y. (2021). The effects of ultrasonic treatment on physicochemical properties and *in vitro* digestibility of semigelatinized high amylose maize starch. *Food Hydrocolloids, 119*, Article 106831.

Chi, C., Li, X., Lu, P., Miao, S., Zhang, Y., & Chen, L. (2019). Dry heating and annealing treatment synergistically modulate starch structure and digestibility. *International Journal of Biological Macromolecules, 137*, 554–561.

Englyst, H., Kingman, S., & Cummings, J. (1992). Classification and measurement of nutritionally important starch fractions. *European Journal of Clinical Nutrition, 46*, 33–50.

Fang, K., He, W., Jiang, Y., Li, K., & Li, J. (2020). Preparation, characterization and physicochemical properties of cassava starch-ferulic acid complexes by mechanical activation. *International Journal of Biological Macromolecules, 160*, 482–488.

Gao, Q., Feng, R., Yu, M., Tao, H., & Zhang, B. (2024). Oleic acid treatment of rice grains reduces the starch digestibility: Formation, binding state and fine structure of starch-lipid complexes. *Food Chemistry, 457*, Article 140191.

Gutierrez, A. S. A., Guo, J., Feng, J., Tan, L., & Kong, L. (2020). Inhibition of starch digestion by gallic acid and alkyl gallates. *Food Hydrocolloids, 102*, Article 105603.
Hao, Z., Han, S., Xu, H., Li, C., Wang, Y., Gu, Z., Hu, Y., Zhang, Q., Deng, C., & Xiao, Y. (2023). Insights into the rheological properties, multi-scale structure and *in vitro* digestibility changes of starch-β-glucan complex prepared by ball milling. *International Journal of Biological Macromolecules, 224*, 1313–1321.
Hao, Z., Xu, H., Yu, Y., Gu, Z., Wang, Y., Li, C., Xiao, Y., Liu, Y., Liu, K., & Zheng, M. (2024). Insights into ball milling treatment promotes the formation of starch-lipid complexes and the relation between multi-scale structure and *in vitro* digestibility based on intermolecular interactions. *Food Hydrocolloids, 146*, Article 109277.
He, H., Chi, C., Xie, F., Li, X., & Chen, L. (2020). Improving the *in vitro* digestibility of rice starch by thermomechanically assisted complexation with guar gum. *Food Hydrocolloids, 102*, Article 105637.
Karunaratne, R., & Zhu, F. (2016). Physicochemical interactions of maize starch with ferulic acid. *Food Chemistry, 199*, 372–379.
Kerr, W. L., Ward, C. D. W., McWatters, K. H., & Resurreccion, A. V. A. (2001). Milling and particle size of cowpea flour and snack chip quality. *Food Research International, 34*(1), 39–45.
Kumar, N., & Pruthi, V. (2014). Potential applications of ferulic acid from natural sources. *Biotechnology Reports, 4*, 86–93.
Li, B., Zhang, Y., Zhao, Y., Luo, W., Huang, C., & Khan, M. R. (2023). Relationship between in vitro digestibility and multi-structures of four unconventional starches from Chinese tropical fruits (sweetsop, avocado, chempedak, and *Pouteria campechiana*) extracted using an ultrasound method. *Industrial Crops and Products, 192*, Article 116011.
Li, B., Zhu, L., Wang, Y., Zhang, Y., Huang, C., Zhao, Y., & Wu, G. (2022). Multi-scale supramolecular structure of *Pouteria campechiana* (Kunth) Baehni seed and pulp starch. *Food Hydrocolloids, 124*, Article 107284.
Li, C. (2023). Starch fine molecular structures: The basis for designer rice with slower digestibility and desirable texture properties. *Carbohydrate Polymers, 299*, Article 120217.
Li, H., Zhai, F., Li, J., Zhu, X., Guo, Y., Zhao, B., & Xu, B. (2021). Physicochemical properties and structure of modified potato starch granules and their complex with tea polyphenols. *International Journal of Biological Macromolecules, 166*, 521–528.
Li, S., Wang, C., Fu, X., Li, C., He, X., Zhang, B., & Huang, Q. (2018). Encapsulation of lutein into swelled cornstarch granules: Structure, stability and *in vitro* digestion. *Food Chemistry, 268*, 362–368.
Li, X., Zhang, Y., Wu, Y., Huang, Y., Huang, X., Wu, Y., Geng, F., Huang, Q., Huang, M., & Li, X. (2024). Divalent metal ions under low concentration environment improved the thermal gel properties of egg yolk. *Poultry Science, 103*(6), Article 103697.
Liu, C., Jiang, Y., Liu, J., Li, K., & Li, J. (2021). Insights into the multiscale structure and pasting properties of ball-milled waxy maize and waxy rice starches. *International Journal of Biological Macromolecules, 168*, 205–214.
Liu, J., Li, X., Jing, R., Huang, X., Geng, F., Luo, Z., … Huang, Q. (2024). Effect of prolonged cooking at low temperatures on the eating quality of Tibetan pork: Meat quality, water distribution, and microstructure. *Food Quality and Safety, 8*, Article fyae025.
Liu, Y., Chen, L., Xu, H., Liang, Y., & Zheng, B. (2019). Understanding the digestibility of rice starch-gallic acid complexes formed by high pressure homogenization. *International Journal of Biological Macromolecules, 134*, 856–863.
Lorentz, C., Pencreac'h, G., Soultani-Vigneron, S., Rondeau-Mouro, C., de Carvalho, M., Pontoire, B., & Le Bail, P. (2012). Coupling lipophilization and amylose complexation to encapsulate chlorogenic acid. *Carbohydrate Polymers, 90*(1), 152–158.
Lu, H., Tian, Y., & Ma, R. (2023). Assessment of order of helical structures of retrograded starch by Raman spectroscopy. *Food Hydrocolloids, 134*, Article 108064.
Lu, T., & Chen, F. (2012). Multiwfn: A multifunctional wavefunction analyzer. *Journal of Computational Chemistry, 33*(5), 580–592.
Lu, X., Wang, Y., Li, Y., & Huang, Q. (2018). Assembly of Pickering emulsions using milled starch particles with different amylose/amylopectin ratios. *Food Hydrocolloids, 84*, 47–57.
Maibam, B. D., Nickhil, C., & Deka, S. C. (2023). Preparation, physicochemical characterization, and *in vitro* starch digestibility on complex of *Euryale ferox* kernel starch with ferulic acid and quercetin. *International Journal of Biological Macromolecules, 250*, Article 126178.
Mancuso, C., & Santangelo, R. (2014). Ferulic acid: Pharmacological and toxicological aspects. *Food and Chemical Toxicology, 65*, 185–195.
No, J., & Shin, M. (2023). Structures and digestibility of B-type high-amylose rice starches compared with A-type high-amylose rice starches. *Journal of Cereal Science, 112*, Article 103713.
Paiva, L. B. D., Goldbeck, R., Santos, W. D. D., & Squina, F. M. (2013). Ferulic acid and derivatives: Molecules with potential application in the pharmaceutical field. *Brazilian Journal of Pharmaceutical Sciences, 49*, 395–411.
Qiu, Z., Chen, L., Rao, C., & Zheng, B. (2023). Starch-guar gum-ferulic acid molecular interactions alter the ordered structure and ultimate retrogradation properties and *in vitro* digestibility of chestnut starch under extrusion treatment. *Food Chemistry, 416*, Article 135803.
Raza, H., Zhou, Q., Cheng, K., He, J., & Wang, M. (2024). Synergistic impact of ultrasound-high pressure homogenization on the formation, structural properties, and slow digestion of the starch-phenolic acid complex. *Food Chemistry, 445*, Article 138785.
Romero Hernández, H. A., Gutiérrez, T. J., & Bello-Pérez, L. A. (2022). Can starch-polyphenol V-type complexes be considered as resistant starch? *Food Hydrocolloids, 124*, Article 107226.
Sun, L., & Miao, M. (2020). Dietary polyphenols modulate starch digestion and glycaemic level: A review. *Critical Reviews in Food Science and Nutrition, 60*(4), 541–555.
Tan, I., Flanagan, B. M., Halley, P. J., Whittaker, A. K., & Gidley, M. J. (2007). A method for estimating the nature and relative proportions of amorphous, single, and double-helical components in starch granules by ^{13}C CP/MAS NMR. *Biomacromolecules, 8*(3), 885–891.
Tian, S., & Sun, Y. (2020). Influencing factor of resistant starch formation and application in cereal products: A review. *International Journal of Biological Macromolecules, 149*, 424–431.
Van Hung, P., Lan Phi, N. T., & Vy Vy, T. T. (2012). Effect of debranching and storage condition on crystallinity and functional properties of cassava and potato starches. *Starch - Stärke, 64*(12), 964–971.
Wang, J., Jiang, X., Guo, Z., Zheng, B., & Zhang, Y. (2021). Insights into the multi-scale structural properties and digestibility of lotus seed starch-chlorogenic acid complexes prepared by microwave irradiation. *Food Chemistry, 361*, Article 130171.
Wang, S., Wang, J., Yu, J., & Wang, S. (2016). Effect of fatty acids on functional properties of normal wheat and waxy wheat starches: A structural basis. *Food Chemistry, 190*, 285–292.
Wang, S., Zheng, M., Yu, J., Wang, S., & Copeland, L. (2017). Insights into the formation and structures of starch-protein-lipid complexes. *Journal of Agricultural and Food Chemistry, 65*(9), 1960–1966.
Yi, X., & Li, C. (2022). Main controllers for improving the resistant starch content in cooked white rice. *Food Hydrocolloids, 122*, Article 107083.
Zhang, H., Qian, S., Rao, Z., Chen, Z., Zhong, Q., & Wang, R. (2021). Supermolecular structures of recrystallized starches with amylopectin side chains modified by amylosucrase to different chain lengths. *Food Hydrocolloids, 119*, Article 106830.
Zhang, P., Huang, X., Fu, C., Gong, Y., Huang, X., Zhang, J., … Huang, Q. (2023). Binding mechanism of Monascus pigment and ovalbumin: Spectral analysis, molecular docking and molecular dynamics simulation. *Food Science of Animal Products, 1*(4), Article 9240038.
Zheng, B., Liu, Z., Chen, L., Qiu, Z., & Li, T. (2022). Effect of starch-catechin interaction on regulation of starch digestibility during hot-extrusion 3D printing: Structural analysis and simulation study. *Food Chemistry, 393*, Article 133394.
Zheng, J., Huang, S., Zhao, R., Wang, N., Kan, J., & Zhang, F. (2021). Effect of four viscous soluble dietary fibers on the physicochemical, structural properties, and *in vitro* digestibility of rice starch: A comparison study. *Food Chemistry, 362*, Article 130181.
Zheng, Y., Tian, J., Yang, W., Chen, S., Liu, D., Fang, H., Zhang, H., & Ye, X. (2020). Inhibition mechanism of ferulic acid against α-amylase and α-glucosidase. *Food Chemistry, 317*, Article 126346.
Zhong, Y., Herburger, K., Xu, J., Kirkensgaard, J. J. K., Khakimov, B., Hansen, A. R., & Blennow, A. (2022). Ethanol pretreatment increases the efficiency of maltogenic α-amylase and branching enzyme to modify the structure of granular native maize starch. *Food Hydrocolloids, 123*, Article 107118.